

Visible and near-infrared silica colloidal crystals and photonic gaps

Dongbin Mei, Hongguang Liu, Bingying Cheng, Zhaolin Li, and Daozhong Zhang
*Optical Physics Laboratory, Institute of Physics and Center for Condensed Matter Physics, Chinese Academy of Sciences,
 Beijing 100080, China*

Peng Dong
National Heavy Oil Research Laboratory, University of Petroleum, Beijing 102200, China
 (Received 3 September 1997; revised manuscript received 7 January 1998)

The transmission spectra at the high-symmetry points of the first Brillouin zone are measured for three face-centered-cubic colloidal crystals made of silica spheres of different submicrometer sizes. It is found that at the U point the transmission dip exists not only for an s wave, but also for a p wave. Moreover, at the W point the transmission dips of both s and p waves appear at the same wavelength. Our calculations confirm that these dips correspond to the lowest band gaps of the high-symmetry points. The structures and parameters of these crystals are determined by the Kossel-rings analysis as well as by the transmission spectra.
 [S0163-1829(98)01926-2]

In the past decade photonic crystals have attracted considerable attention.¹ Because of the existence of photonic gaps, the properties of light propagation and the interaction between atoms or molecules may be substantially modified,²⁻⁷ which may lead to many potential applications for electro-optic devices. One exciting area is the construction of photonic crystals that are effective in the near-infrared or visible region. Recently, many investigations have addressed the formation of three-dimensional dielectric structures with a submicrometer lattice constant. Tarhan and Watson and Vos *et al.* created, respectively, polystyrene and silica colloidal face-centered-cubic (fcc) crystals, while Vlasov *et al.* observed the pseudogap in synthetic opals.⁸⁻¹¹ It is quite remarkable that the transmission measurement at the W point performed by Tarhan and Watson gave a different result compared with a previous theoretical calculation, i.e., the degeneracy of p and s waves at the W point for a fcc crystal with dielectric spheres was not found.¹² To find out if this discrepancy is specific for the colloidal crystal made of polystyrene spheres or is a common feature of colloidal crystals, we measured the transmission spectra at the high-symmetry points of the first Brillouin zone, namely, L , $[(2\pi/a)(\frac{1}{2}, \frac{1}{2}, \frac{1}{2})]$; X , $[(2\pi/a)(1, 0, 0)]$; U , $[(2\pi/a)(1, \frac{1}{4}, \frac{1}{4})]$; W , $[(2\pi/a)(1, \frac{1}{2}, 0)]$, for three colloidal crystals made of silica spheres with diameters 0.2, 0.33, and 0.46 μm , respectively. The structure and main parameters of the silica colloidal crystals are determined by the Kossel-rings analysis, as well as by the transmission spectra. The major results reported here are summarized as follows. At the L point the transmittance drops rapidly as the incident wavelength decreases. At the U point a transmission dip exists not only for an s wave, but also for a p wave, and at the W point the transmission dips of both s and p waves appear for the same wavelength. Our band-gap calculations confirm that these dips correspond to the lowest gaps at the different high-symmetry points.

The submicrometer monodisperse silica spheres were prepared by hydrolysis and condensation of tetraethoxysilane in

a mixture of water, ammonia, and ethanol. The sphere size was controlled by the nuclei scale and their growth time.¹³ The spheres obtained were separated by centrifugation and washed several times with doubly distilled water to remove all solutes. The $p\text{H}$ value of the final suspension was selected to be more than 7, i.e., weak alkaline. We fabricated three kinds of silica spheres of diameters 0.2, 0.33, and 0.46 μm , respectively, with standard deviation less than 5%. The colloidal crystals were grown through gravitation sedimentation in two types of rectangular quartz cuvettes of thickness 1 and 0.4 mm, respectively. The thicker ones are for the larger spheres of 0.33 and 0.46 μm diameter, while the thinner cuvette is for 0.2- μm spheres. The time for the formation of a colloidal crystal depends strongly on the sphere size. The larger the sphere the shorter the time required. It took three weeks or so to form a 10-mm-high colloidal crystal for 0.33- and 0.46- μm spheres, while it took at least six weeks for 0.2- μm spheres. This is mainly caused by the slow sedimentation speed of smaller spheres. At the end of this period the iridescence of the whole crystal could be seen. However, the structure of newly formed colloidal crystals is not stable, especially for those made of larger spheres. At the beginning the lattice constant in the upper and bottom areas of the sample is different, though they possess the same fcc structure. For example, their ratio can be as large as 1.04 for the crystal with 0.33- μm spheres. Fortunately, it can be gradually and naturally reduced to close to 1 in the ensuing 12 weeks under the action of gravity and electrostatic forces. After that the structure parameters do not change. We have tried to shorten the sedimentation time by using centrifuging, but this method cannot ensure the fcc structure of the sample. The silica fraction of a formed crystal is related to the size of the spheres and the $p\text{H}$ value of the suspension. Under our experimental conditions the volume fractions of the silica spheres f in the crystals of 0.33- and 0.46- μm spheres vary between 0.45 and 0.6, while for the crystal with 0.2- μm spheres it is between 0.3 and 0.4, determined by Kossel-rings analysis and the transmission spectra.

In the determination of crystal structure by Kossel-ring analysis, the orientations and spacings of major crystal planes were simultaneously derived. The principle of this method is rather simple.^{8,14,15} When a divergent laser beam passes through a colloidal crystal, the scattering of light is anisotropic due to Bragg diffraction. The beam propagating along the Bragg-diffraction cone will be diffracted, so that dark rings exist in the transmission. Different crystal planes have different rings and the axis of each ring is normal to the corresponding diffraction planes. From the half-angular width of each ring ϕ , the crystal plane spacing d may be derived by $d = \lambda/2n_e \cos \phi$, where λ and n_e are the incident wavelength and effective refractive index of the crystal, respectively. Previous studies have pointed out that in the case of fraction $f < 0.7$ the Maxwell-Garnett theory can give a suitable effective dielectric constant for a fcc crystal, i.e., $\varepsilon_e = \varepsilon_1[2\varepsilon_1 + \varepsilon_2 + 2f(\varepsilon_2 - \varepsilon_1)]/[2\varepsilon_1 + \varepsilon_2 - 2f(\varepsilon_2 - \varepsilon_1)]$, where $\varepsilon_2 = 2.1$ and $\varepsilon_1 = 1.77$ are the dielectric constants of the spheres and surrounding water, respectively.¹⁶ This expression pertains only to the limit of the wave vector $k \rightarrow 0$. However, previous⁹ and present experimental results show that it is quite good for silica colloidal crystals.

We observed the Kossel-ring distributions for three colloidal crystals *C1*, *C2*, and *C3*, made of silica spheres 0.2, 0.33, and 0.46 μm in diameter, respectively. The following common characteristics can be derived. (1) All of them have the fcc structure. (2) Their (111) planes (the densest plane of silica spheres) are parallel to the surface of the cuvette. (3) The normals of the (111) and (002) planes are in a plane that is perpendicular to the surface of the cuvette. The third characteristic is not the same as in Tarhan and Watson's polystyrene experiment, where the normal to the (002) planes was not perpendicular to the cuvette surface.¹⁰ It should also be noted that though the three crystals have the same characteristics as described above, the observed ring distributions are quite different. In the cases of *C1* and *C2* (the crystals with smaller size spheres) the rings originating from the (111), (002), and (020) planes may be clearly identified, while for the crystal of 0.46- μm spheres, instead of rings from the (002) and (020) planes, we saw rings from the (111), (311), and (131) planes. In addition, the appearance and iridescence of the crystals are different, too. The *C1* crystal looks uniform and transparent. The color of its iridescence changes continuously, like the diffraction for a grating, when the crystal is rotated. One cannot see the flashing lines under sunlight. In the case of *C2* and *C3* crystals, however, there is a certain amount of discrete flashing points and lines. This may be an indication that the micropolycrystal structure or different kinds of defects in the *C2* and *C3* crystals are denser than in the *C1* crystal. Based on the Kossel-ring observations the spacings between the (111), (002), or (311) planes can be derived. The corresponding lattice constant a and volume fraction of the sphere f for these three crystals are obtained to be $a \sim 364, 524, \text{ and } 805 \text{ nm}$, and $f \sim 0.36, 0.52, \text{ and } 0.46$ for *C1*, *C2*, and *C3*, respectively. To make sure that the measured fraction is reliable, we finally weighed the dried sample of 0.33- μm spheres and obtained a fraction of ~ 0.5 , which is slightly less than the 0.52 of our optical measurement. This is because a small amount of silica spheres became attached strongly to the inner surface of the cuvette during the heating process. Furthermore, from the

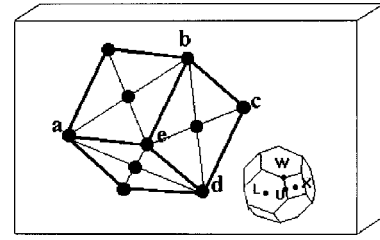


FIG. 1. Relative orientation of the colloidal crystal and the high-symmetry points of the first Brillouin zone with respect to the cuvette. The (abd) plane, i.e., the (111) plane of the fcc crystal, is parallel to the front surface of the cuvette and the line (ec) is parallel to the base.

spatial arrangement of the colloidal crystals inside the cuvette the orientations of the high-symmetry points of the fcc crystals may be immediately determined, as shown schematically in Fig. 1.

The transmission spectra at the L , X , U , and W points were measured by two spectrometers: a Cary2390 spectrophotometer for the *C1* crystal in the visible region and a Bio-Rad FTS-6000 spectrometer for the *C2* and *C3* crystals in the near-infrared region. To achieve the required angle of incidence in the colloidal crystal the cuvette was embedded in a small glass cylinder filled with water. The main results for sample *C1* are shown in Fig. 2. At the L point, i.e., incident angle of 0° , a sharp dip about $\sim 30 \text{ nm}$ wide appears around 561 nm in the spectrum of Fig. 2(a), while the transmittance T drops down as the wavelength λ decreases. In the opal sample Vlasov *et al.* found a similar decrease and they fitted the transmission curve in terms of λ^4 dependence.¹¹ This kind of transmitted intensity drop has also been observed in far-infrared two-dimensional photonic crystals, caused possibly by defects or disorder in the crystals.^{17,18} It is well known that for an assembly of random particles with a size less than a light wavelength, the scattering intensity decreases with the fourth power of wavelength. However, in the case of opal and colloidal crystal samples most of the silica spheres have been arranged to form an fcc structure and, moreover, from the observation of the Kossel rings and the transmission dip, the (111) planes have the best ordered structure (the sharpest ring and dip). Therefore, in principle, the λ^4 dependence should not be a suitable fit. To understand this phenomenon we have calculated and plotted the dependencies of T on both λ^4 and λ^5 , respectively, as the dashed and dotted line in Fig. 2(a). It can be seen that the λ^5 dependence seems to be more likely, except for wavelength shorter than 400 nm. The difference in the short-wavelength region might be due to the second gap of the L point, which should be located at around 295 nm according to our calculation. In addition, the transmission spectrum and both λ^4 and λ^5 dependencies at the L point of *C3* colloidal crystal (with 0.46- μm spheres) are plotted in the inset of Fig. 2(a). As we have described in the previous paragraph, the defects in the *C3* crystal are much more numerous than in the *C1* crystal. Even so, the variations of T with the wavelength are almost the same for both *C1* and *C3* colloidal crystals. This might imply that, besides the defects or disorder of the crystal, there is another cause for this phenomenon. The study of coherent x-ray scattering of atomic crystals has pointed out that because the x-ray wavelength and the size of atom have

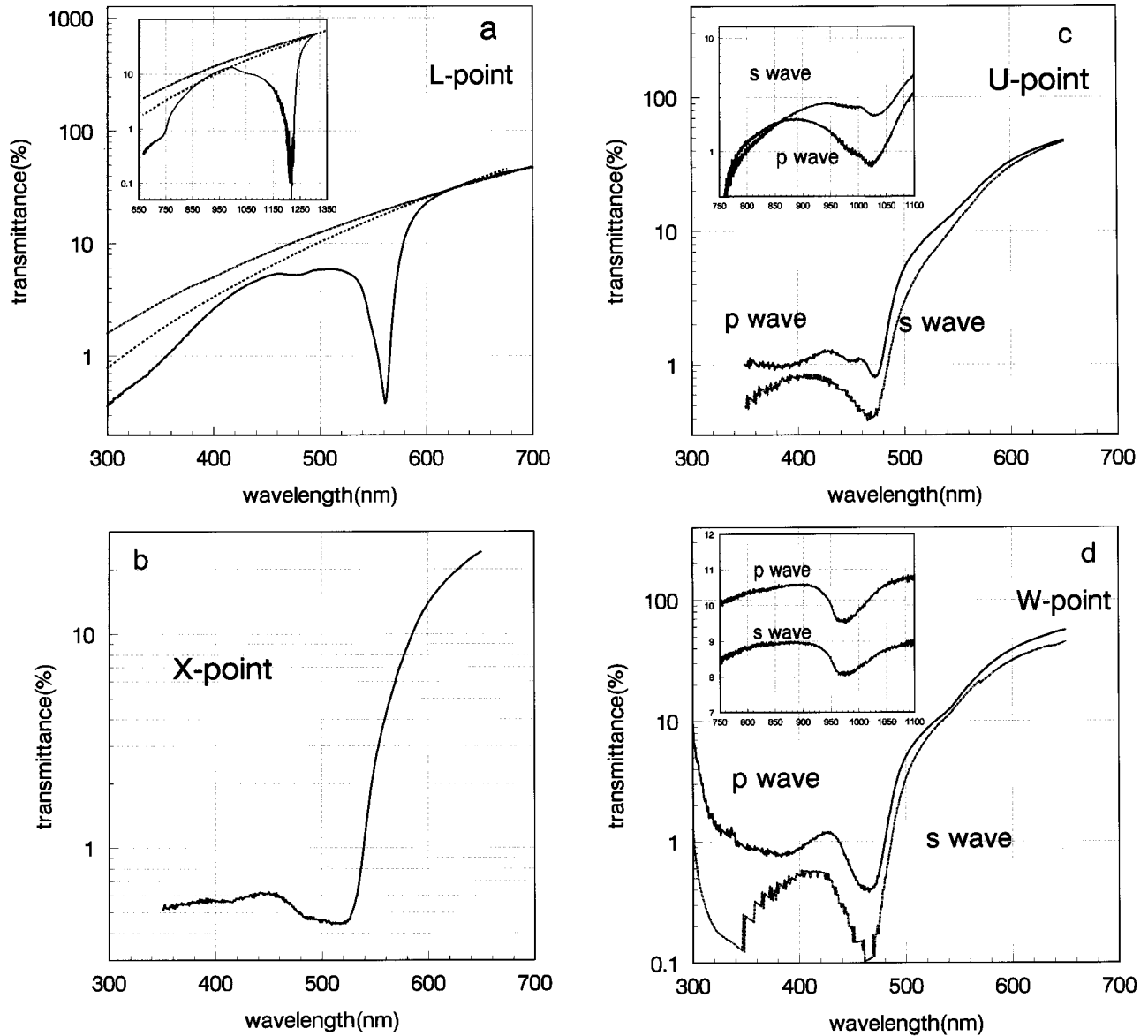


FIG. 2. Transmission spectra of the fcc colloidal crystal with $0.2\text{-}\mu\text{m}$ silica spheres ($C1$ crystal) at four high-symmetry points of the first Brillouin zone. (a) The L point. Dashed line, $T\alpha\lambda^4$; dotted line, $T\alpha\lambda^5$. Inset: Corresponding curves for the $C3$ crystal. (b) The X point. (c) The U point for two polarized incident waves. Inset: Transmission spectra of the U point for the $C3$ crystal. (d) The W point for both p and s waves. Inset: Transmission spectra of the W point for the $C3$ crystal.

the same order of magnitude, the phase of the scattered waves from different electrons of atoms are not the same. Thus, the atomic-scattering factor can be strongly related to the incident x-ray wavelength, i.e., the scattered intensity is no longer a constant as wavelength changes.¹⁹ In the transmission measurement of current photonic crystals the situation is very similar, since the wavelength of the light is comparable with the submicrometer size of the silica spheres. Therefore, the phases of the scattering light waves coming from the different parts of sphere's surface are not identical. The coherence between these scattered light waves is thus related to the light wavelength, which leads to a dependence of scattering intensity, as well as the transmittance, on λ . This effect may be the major cause for the intensity variation with the wavelength. A quantitative explanation is under consideration. Furthermore, from the dip position of the L point, ~ 561 nm, the corresponding lattice constant

$a = 355$ nm is obtained, which agrees reasonably with the value of 364 nm determined by the Kossel-rings method.

The measurements were then carried out by changing the incident angle θ , step by step, between 0° and 54° , corresponding to the variation of the incident wave vector along $L(0^\circ) - U(35^\circ) - X(54^\circ)$. It is found that as the incident angle increases, the observed transmission dip becomes wider and shallower, shifting towards short wavelengths for $\theta < 35^\circ$ and back to longer wavelengths for $35^\circ < \theta < 54^\circ$. At the X point there is a rather shallow dip around 517 nm with a width more than 60 nm [Fig. 2(b)]. In the above experiments an unpolarized beam was used. However, due to the spatial symmetry of the fcc structure the polarization should be considered for the transmission measurements at the U and W points.¹² Figure 2(c) shows the spectra of the U point for an s wave (the electric vector perpendicular to the incident plane, which is perpendicular to the cuvette front sur-

face and parallel to the cuvette base) and p wave (in the incident plane), respectively. The curves for the s and p waves have the same transmission minimum of ~ 472 nm, though their depths are slightly different. To make the issue clearer, the corresponding transmission spectra between 750 and 1100 nm of the $C3$ crystal are plotted in the inset of Fig. 2(c). The p -wave dip is more obvious, which means that at the U point the lowest p -wave gap is open too for the $C3$ crystal. The transmittance decrease in the shorter wavelength for the $C3$ crystal is more rapid than for the $C1$ crystal. This might be partly attributed to the greater number of defects in the $C3$ crystal. This observation is quite interesting, because based on the calculation given by Ho *et al.* the first gap at the U point is closed for a p wave and open only for an s wave.¹² The measured results of the W point of the $C1$ crystal are plotted in Fig. 2(d), where the spectra for two polarized waves are very close and their dips, both around 460 nm, almost overlap with each other. In the inset of Fig. 2(d) the transmission spectra at the W point of the $C3$ crystal are given, from which it can be seen that the shapes of both curves are very similar, although the transmittances are slightly different. It should be noted that in the measurement of the W point the cuvette was tilted by 18.5° with respect to the L - X - U plane, while the polarization of the beam was unchanged. A similar effect was also found in the fcc polystyrene colloidal crystal by Tarhan and Watson.⁸ Moreover, at the W point there is a second broad dip around 350 nm for both s and p waves and the dip of the s wave is much deeper than that of the p wave, while in Ref. 8 both dips are nearly the same. This might correspond to the second gap at the W point. The phenomena occurring at the U and W points of the $C1$ crystal were observed in the $C2$ crystals, too. To know if the measured dips are indeed related to the corresponding photonic gaps, a simple band-gap calculation (the polarization of the incident beam was not taken into account) of the $C1$ and $C3$ crystals were performed by the plane-wave expansion of the magnetic vector with 343 basis waves. Though the number of basis waves is small, the positions of the lowest gaps at the L , X , U and W points can still be obtained with an accuracy of $\sim 3\%$. The agreements

TABLE I. Comparison of the positions between measured dips and calculated gaps at four high-symmetry points of the first Brillouin zone (L , X , U , and W) for two crystals composed of 200-nm ($C1$) and 460-nm ($C3$) silica spheres, respectively.

	L	X	U	W
$C1$, meas. (nm)	561	500	472	450
$C1$, calc. (nm)	574	517	472	460
$C3$, meas. (1/cm)	8190	9410	9800	10 300
$C3$, calc. (1/cm)	8150	9430	9980	10 500

between calculation and measurement of the gap position are reasonably good, as shown in Table I. Thus, our measurements at the U and W points mean that the discrepancy between experiments and previous calculation of a perfect fcc photonic crystal exists for our silica colloidal crystals, too. This seems to be a common feature of colloidal crystals, for which the reason is not fully clear. Sigalas *et al.* calculated the transmission spectra of the disordered two-dimensional photonic crystals and found that the disorder may seriously affect the spectrum.²⁰ A detailed light-propagation calculation for a three-dimensional photonic crystal, in which disorder is taken into account, is therefore necessary for understanding the above experimental results. This kind of calculation may also indicate if any uncoupled mode exists or not.²¹

In conclusion, we have prepared three silica fcc colloidal crystals and determined their structural parameters, while their transmission spectra have been measured in the visible and near-infrared region. In terms of the coherence between scattered-light waves coming from different parts of sphere's surface, the transmittance decrease with the decrease of wavelength at the L point may be qualitatively understood. The experimental results, which do not coincide with previous calculation, have been also observed at the U and W points of our silica colloidal crystals. Further study is needed for finding the reason for this.

The authors are grateful to the National Natural Science Foundation of China for financial support.

¹For example, *Photonic Band Gaps and Localization*, edited by C. M. Soukoulis (Plenum, New York, 1993); *Photonic Band Gap Materials*, edited by C. M. Soukoulis (Kluwer, Dordrecht, 1996).

²E. Yablonovitch, Phys. Rev. Lett. **58**, 2059 (1987); **67**, 2295 (1991).

³J. Martorell and N. M. Lawandy, Phys. Rev. Lett. **65**, 1877 (1991).

⁴T. Suzuki and Paul K. L. Yu, J. Opt. Soc. Am. B **12**, 804 (1995).

⁵S. John and T. Quang, Phys. Rev. Lett. **76**, 1320 (1996); **76**, 2484 (1996).

⁶E. Ozbay, J. Opt. Soc. Am. B **13**, 1945 (1996).

⁷D. F. Sievenpiper *et al.*, Phys. Rev. Lett. **76**, 2480 (1996).

⁸I. I. Tarhan and G. H. Watson, Phys. Rev. Lett. **76**, 315 (1996).

⁹W. L. Vos *et al.*, Phys. Rev. B **53**, 16 231 (1996).

¹⁰W. L. Vos *et al.*, J. Phys.: Condens. Matter **8**, 9503 (1996).

¹¹Yu. A. Vlasov *et al.*, Phys. Rev. B **55**, R13 357 (1997).

¹²K. M. Ho *et al.*, Phys. Rev. Lett. **65**, 3152 (1990).

¹³Shengli Chen *et al.*, J. Colloid Interface Sci. **180**, 237 (1990).

¹⁴R. J. Carlson and S. A. Asher, Appl. Spectrosc. **38**, 297 (1984).

¹⁵T. Yoshiyama and I. Sogami, in *Ordering and Phase Transitions in Charged Colloidal*, edited by A. K. Arora and B. V. R. Tata (VCH, New York, 1996).

¹⁶S. Datta *et al.*, Phys. Rev. B **48**, 14 936 (1993).

¹⁷M. Wada *et al.*, Phys. Rev. B **52**, 16 297 (1995).

¹⁸Hongqiang Li *et al.*, Phys. Rev. B **56**, 10 734 (1997).

¹⁹A. H. Compton and S. K. Allison, *X-ray in Theory and Experiment* (Macmillan, London, 1935), Chap. 3.

²⁰M. Sigalas *et al.*, Phys. Rev. B **53**, 8340 (1996).

²¹K. Sakoda, Phys. Rev. B **55**, 15 345 (1997).